Super Resolution of License Plates Using Generalized DAMRF Image Modeling

Vikas Nivrutti Dhakane [1], Jalinder Nivrutti Ekatpure[2]

Assistant Professor, Solapur University, SMSMPITR College of Engineering, Akluj, Solapur, Maharshtra, India

Abstract: ***LPR (License Plate Recognition) is a main component of modern transportation management systems. It uses a set of computer image-processing technologies to identify vehicles by its license plate. We propose a novel super resolution (SR) reconstruction algorithm to handle license plate texts in real traffic videos. To make license plate numbers more legible, a generalized discontinuity-adaptive Markov random field (DAMRF) model is proposed based on the recently reported bilateral filtering, which not only preserves edges but is robust to noise as well. Moreover, instead of looking for a fixed value for the regularization parameter, a method for automatically estimating it is applied to the proposed model based on the input images. Information needed to determine the regularization parameter is updated at each iteration step, which is based on the available reconstructed image. Character recognition is the core of LPR.***

Keywords: Bilateral filter, Markov Random Field (MRF), Maximum *A Posteriori* (MAP), regularization, Super Resolution (SR).

1. Introduction

1.1 Introduction to LPR Application

Vehicle detection is very important for civilian and military applications, such as highway monitoring, and the urban traffic planning. Vehicles detection must be implemented at different environment where the light and the traffic status changing. Loop detectors are considered as point detectors and could not give the traffic information for the highway. Vision based techniques are more suitable than the magnetic loop sensors. They do not disturb traffic while installed and they are easy to modify. Their applicability is more comprehensive because they could be used in many aspects as vehicle detection, counting, classification, tracking, and monitoring. One camera could be used to monitor large section of highway. In spite the apparent advantages of vision based methods there are still many challenges. These challenges are weather changes, sun light direction and intensity changes, building shadows, vehicles have different sizes, shapes and colors. In this paper one [1].

1.2 Purpose of LPR Application

In these approaches the background is not extracted but detected and then updated through the next images Processing. Intensity changes, stopped vehicles (or very slow moving vehicles) and camera moving lead to miss detection in these techniques. It is used to detect vehicle in simple scenes. Another approach uses edge-based techniques. In this approach 2D model is proposed for the vehicle. This 2D model depends on the edge detection of the vehicle. It is applicable under perfect conditions for passenger vehicles only. The edge in image processing is abrupt change in the intensity values [1].

2. Analysis of the System

2.1 Existing System

The LPR algorithm was used as the existing algorithm, The LPR algorithm consists of two modules, one for locating license plates and one for identifying license numbers. Soft computing techniques rooted in fuzzy (for license plate location) and neural (for license number identification). The Existing algorithm is concerned with the license plates of one specific country, many parts in the algorithm are readily extended to use with license plates of other countries. Specifically, since color and edge are two fundamental features of license plates, the color edge detector introduced in the locating module is readily adapted to other color schemes by replacing the color parameters embedded in the detector [2].

2.2 Proposed System

An algorithm for license plate recognition (LPR) applied to the intelligent transportation system is proposed on the basis of a novel shadow removal technique and character recognition algorithms. This paper has two major contributions. One contribution is a new binary method, i.e., the shadow removal method, which is based on the improved Bernsen algorithm combined with the Gaussian filter. This paper also presents improved techniques for image tilt correction and image gray enhancement. Our algorithm is robust to the variance of illumination, view angle, position, size, and color of the license plates when working in a complex environment [1].

2.3 Analysis of Typical Parts of the System

A typical system for LPR consists of following parts [1], [2]:

2.3.1 License Plate Localization

Localizing is an algorithmic function that determines what aspect of the vehicle's image is the license plate. In general, algorithms look for geometric shapes of rectangular proportion. However, since a vehicle can have many rectangular objects on it, further algorithms are needed to validate that the identified object is indeed a license plate. To accomplish this, key components of the algorithm look for characteristics that would indicate that the object is a license plate. The algorithm searches for a similar background color of unified proportion and contrast as a means to differentiate objects on a vehicle. Vehicles are moving objects and their rate of velocity must be accounted for in the algorithm's

design. This speed creates further complexity as a license plates image is angularly skewed and subjected to refractory issues from light changes. External hardware components and filters may be used to control for light fluctuation.

2.3.2 License Plate Sizing and Orientation
Components of algorithms that adjust for the angular skew of the license plate image to accurately sample, correct, and proportionally recalculate to an optimal size.

2.3.3 Normalization
Algorithm for regulating the contrast and brightness of the captured license plate image.

2.3.4 Character Segmentation
Algorithm that locates the separate alpha numeric characters on a license plate. Algorithms also look for characters of equal color and equidistance, with similar font structures to break apart each individual character. This sequential congruency of the characters embodies a characteristic set that is typically uniform, regardless of the type of license plate. Character Segmentation separates each letter or number where it is subsequently processed by optical character recognition (OCR) algorithms.

2.3.5 Optical Character Recognition in LPR
Algorithm for translating the captured image into an alpha numeric text entry.

2.3.6 Syntactical and Geometrical Analysis
Algorithm to verify alpha numeric information and arrangement with a specific rule set. The algorithms operate sequentially with instructions being executed in milliseconds. The successful completion of each algorithm is required before subsequent algorithms can be operational.

3. SR Algorithms

Generally, the SR algorithm can be divided into two categories:1) frequency-domain algorithms 2) spatial-domain algorithms. For the frequency-domain algorithms, proposed work is to enhance the resolutionof multitemporal Landsat thematic mapper (TM) images by estimating the relative shifts between observations. However, the frequency-domain methods seldom incorporate prior knowledge and can only be applied to translation motion, which limited their applications. For this reason, a wide variety of spatial-domain SR reconstruction methods have been developed for recent years [3], [4], [5], [6], [7], [8]. In [4], A Bayesian SR algorithmic developed based on the simultaneous autoregressive model, which is tested on two sets of real text images and car plates. A neural-network-based method has been proposed in to perform SR of license plates with lower computational needs. Machine-learning based framework is used to zoom the digits in a license plate. These methods introduce smoothness constraints to suppress the noise in reconstructed images, but it loses some details in HR images. More recently, a discontinuity-adaptive Markov random field (MRF) SR method is proposed, in which the HR image is modeled as MRF with discontinuity-adaptive regularization, and a maximum *a posteriori* (MAP) estimate of the super resolved image is obtained, given the low-quality image sequence.

The proposed discontinuity-adaptive MRF (DAMRF) model gets promising results in some cases when tested on real traffic video sequences. However, this method is not locally adaptive, and therefore, it has limited adaptive capability in the process of SR reconstruction and cannot balance the preservation of image details against the suppression of noise. To reduce the shortcomings of the aforementioned DAMRF method, in this paper, we proposed a generalized DAMRF (GDAMRF) model based on bilateral filtering, which connects bilateral filtering with the Bayesian MAP. Regularization parameter is updated at each iteration step based on the available reconstructed image. The organization of the rest of the paper is given as follow.

4. Problem Simulation

4.1 Observation Model

Given that we observe n LR images$\overrightarrow{Y1}, \overrightarrow{Y2},\ldots.\overrightarrow{Yn}$ we use the notation in [9] to formulate the general SR observation model. The degraded sequence of the original image is assumed to be translational with scaling-variant motions. The blurring comes from camera defocus, atmosphere, and motion blur. The general vector SR formulation is defined as

$$\overrightarrow{Y}_k = D_k B_k F_k \overrightarrow{X} + \overrightarrow{W_k}, \quad 1 \le k \le n \quad (1)$$ Where

$\overrightarrow{X}$ HR image of size $[N_1N_2 \times 1]$, which is rearranged in Lexicographic order;

$\overrightarrow{Y_k}$ kth input LR frame of size $[M_1M_2 \times 1]$, which is Rearranged in lexicographic order;

B_k camera lens blur matrix of size $[N_1N_2 \times N_1N_2]$;
F_k geometric motion operator of size $[N_1N_2 \times N_1N_2]$;
D_k decimation matrix of size $[M_1M_2 \times N_1N_2]$;
$\overrightarrow{W_k}$ Additive noise of size $[M_1M_2 \times 1]$.

Recovery of image $\overrightarrow{X}$ from $\{\overrightarrow{Y}_k\}_{nk=1}$ relies on the knowledge of the involved operators. By setting the center frame as a reference image, operator F_k is obtained through motion estimation between the reference image and image $\overrightarrow{Y}_k$. Therefore, $\forall k, D_k = D$, and $B_k = B$.

4.2 SR Based on the MRF-MAP Model

To compute an estimate of the HR image$\vec{X}$, given that we Observe n LR images. The MAP estimate can be computed a

$$X = \arg\max_{\overrightarrow{X}} \left\{ P(\overrightarrow{X} | \overrightarrow{Y}_1, \ldots, \overrightarrow{Y}_n) \right\} \quad (2)$$

This function can be computed using Bayes' rule, with

$$X = \arg\max_{\overrightarrow{X}} \left\{ \frac{P(\overrightarrow{Y}_1, \ldots, \overrightarrow{Y}_n | \overrightarrow{X}) P(\overrightarrow{X})}{P(\overrightarrow{Y}_1, \ldots, \overrightarrow{Y}_n)} \right\}$$

Taking the logarithm of the aforementioned posterior probability, we obtain

$$X = \arg\max_{\vec{X}} \left\{ \log P(\vec{Y}_1, \ldots, \vec{Y}_n | \vec{X}) + \log P(\vec{X}) - \log P(\vec{Y}_1, \ldots, \vec{Y}_n) \right\}$$

Since the third term of the log-likelihood function is not dependent On $\vec{X}$, it can be eliminated from the optimization equation. The MAP estimate of $\vec{X}$, can then be written as

$$X = \arg\max_{\vec{X}} \left\{ \log P(\vec{Y}_1, \ldots, \vec{Y}_n | \vec{X}) + \log P(\vec{X}) \right\}. \quad (3)$$

To compute MAP estimation, we have to define the conditional density $P(\vec{Y}_1 \ldots \vec{Y}_n | \rightarrow X)$ and the density $P(\vec{X})$.Note that, in the observed model (1), $P(\vec{Y}_1, \ldots, \vec{Y}_n | \vec{X}) = P(\vec{W}_k)$. (4) we have As well known, Gaussian noise is used to model the thermal properties of charge-coupled-device image acquisition sensors [10], and therefore, we assume that the noise is a white Gaussian noise. Using the fact that the noise fields are statistically independent of as well as each other, we have

$$P(\vec{Y}_1, \ldots, \vec{Y}_n | \vec{X}) = \frac{1}{(2\pi\sigma^2)^{\frac{nM_1M_2}{2}}} \exp\left\{ -\sum_{k=1}^{n} \frac{\| \vec{Y}_k - DBF_k \vec{X} \|_2^2}{2\sigma^2} \right\} \quad (5)$$

Where $\sigma 2$ is the variance of the observation noise. To model the image, an MRF is assumed with the Gibbs density function, i.e.,

$$P(\vec{X} = \vec{x}) = \frac{1}{Z} \exp\left\{ -\frac{1}{T} \sum_{c \in C} V_c(\vec{x}) \right\} \quad (6)$$

where Z is a normalized constant, T is the "temperature" Parameter of the density, $V_c(\cdot)$ is some function of a local group of points c, and C denotes the set of all cliques throughout the image [8], [9], [10], [11].

5. Generalized Discontinuity Markov Random Field Model

In this section, we first proposed a GDAMRF model for image SR and then discuss three implement issues. Finally, we use the graduated no convexity (GNC) algorithm for performing optimization.

5.1 GDAMRF Prior Model Based on Bilateral Filter

The prior model (3) plays a very important role in the SR reconstruction process. In a variety of applications, it is necessary to remove additive noise and smooth an image while preserving its edges. As we know, bilateral filtering was proposed as a popular tool to reduce noise and preserve edges by means of exploiting all relevant neighborhoods [12]. It combines gray levels based on not only their gray similarity but on their geometric closeness as well and prefers near values to distant values in both domain and range. Recently, many authors have been devoted to bilateral filtering [13], [14], [15], [16]. In [13], Barash established the bridge with adaptive smoothing and anisotropic diffusion. In [14], Farsiu *et al.* proposed a robust SR method using L1 norm minimization and robust regularization based on bilateral filtering but with limited success. Elad [15] proposed a link between the bilateral filtering and the Bayesian approach and showed that a single iteration of the Jacobi algorithm yields bilateral filtering. Still, Elad [16] proposed a new penalty function via bilateral filters for Retenex theory, which suppress noise and deals with better edges. Based on the reported bilateral filters, we introduce the following generalized MRF prior model. Hence, the MRF prior model (3) can be alternatively written as

$$P[\vec{X} = \vec{x}] = \frac{1}{Z} \exp\left\{ -\frac{1}{T} V_c(\vec{x}) \right\} \quad (7)$$

Where

$$V_c(\vec{x}) = \sum_{c \in C} \sum_{a \in N_c} d(a,c) s(\vec{x_a}, \vec{x_c}) \quad (8)$$

With $d(a, c)$ and $s(\vec{x}\, a, \vec{x}\, c)$ being the geometric closeness and photometric similarity, respectively, between the neighborhood center c and a nearby point a. How to choose the closeness function $d(a, c)$ and the similarity function $s(\vec{x}\, a, \vec{x}\, c)$ is crucial to the quality of the reconstructed image. A simple and common choice for the closeness function is the Gaussian function of the Euclidean distance between their arguments [11], i.e.

$$d(a,c) = \exp\left\{ -\frac{1}{2} \left(\frac{\|a - c\|}{\sigma_d} \right)^2 \right\} \quad (9)$$

Where $\|\cdot\|$ is the Euclidean distance. The spread σ_d must be adjusted accordingly to obtain the desired results. A large σ_d combines values from more distant image locations, which means more blur. As for the similarity function, it is crucial to the quality of the reconstructed image. We choose it to be of the form

$$s(\vec{x}_a, \vec{x}_c) = g(\vec{x}_a - \vec{x}_c) \quad (10)$$

The property of this function is that it should be adaptively adjusted between pixels across edges to preserve discontinuities, i.e., wherever a discontinuity occurs, the interaction would diminish. For any regularization model to be adaptive to discontinuities, it should satisfy the following property

$$\lim_{\eta \to \infty} |g'(\eta)| = \lim_{\eta \to \infty} |2\eta f(\eta)| = C \quad (11)$$

where $C \in [0, \infty)$ is a constant, and $f(\cdot)$ is called an interaction function. Interaction $f(\eta)$ must be small for large $|\eta|$ and approaches 0 as $|\eta|$ goes to ∞. Based on previous guidelines, [17] defined an adaptive interaction function $f_\gamma(\eta)$ parameterized by $\gamma(> 0)$ and satisfies the following five properties:

1. $f\gamma(\eta) > 0$ (no negativity);
2. $f\gamma(\eta) = f\gamma(-\eta)$ (symmetric);
3. $f\_\gamma(\eta) < 0$ (monotonicity);
4. $f\gamma(\eta) \in C1$ (continuously differentiability);

Moreover, Li [17] developed four functions of the adaptive potential function, which satisfy the five aforementioned properties. Among these, we use one of them, and it is defined as where parameter $\gamma(> 0)$ controls the shape of the function. Fig. 5.1 shows the DA g-function and its first derivation h-function. The h-function is given by

$$h(\vec{x}_a - \vec{x}_c) = 2\|\vec{x}_a - \vec{x}_c\| \exp\left(-\|\vec{x}_a - \vec{x}_c\|^2/\gamma\right) \quad (13)$$

In terms of (5) and (11), (6) can be equivalently written as follows:

$$V_\gamma(\vec{X}) = \sum_{c\in C}\sum_{a\in N_c} \exp\left\{-\frac{1}{2}\left(\frac{\|a-c\|}{\sigma_d}\right)^2\right\} \times \left\{\gamma - \gamma \exp\left(-\|\vec{x}_a - \vec{x}_c\|^2/\gamma\right)\right\} \quad (14)$$

By using the MAP estimation, the conditional density in (18), and the image model in (4), we propose the following DAMRF model:

$$F(\vec{X}) = \arg\min_{\vec{X}} \left\{\sum_{k=1}^{n} \|\vec{Y} - DBF_k\vec{X}\|_2^2 + \lambda V_\gamma(\vec{X})\right\} \quad (15)$$

Where $\lambda = \sigma_2/T$ is the regularization parameter that provides a tradeoff between the constrain $V_\gamma(-\rightarrow X)$ and the error term.

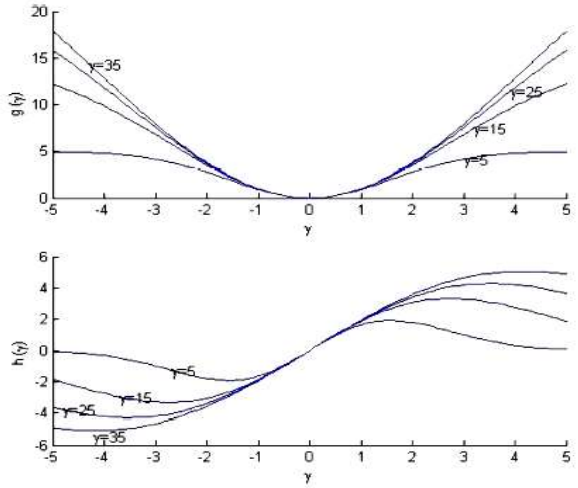

Figure 5.1: DA *g*-function and DA *h*-function for different γ values (γ = 5, 15, 25, 35).

5.2 Implementation Issues

Solving GDAMRF model (19) involves three implementation issues

1. Get input$\vec{Y}1,\vec{Y}2, \ldots ,\vec{Y}n,$ which has been cropped by a text detection process. Many algorithms can be used to solve it [20]
2. Estimate motion parameters for the image sequence. Accurate motion estimation of these images plays an important role in the performance of the SR algorithms. In this paper, we used two-step approach to register each of the sequence with respect to the reference image: de-blurring prior to the motion estimate and computation of rough translational motion from scale-invariant key point matching. The first step is relatively simple and conventional, which can be done in various ways [21]. The second step uses scale invariant feature transform and a Gaussian pyramid data structure to register the sequence.
3. The regularization parameter controls the tradeoff between fidelity to the data and smoothness of the solution. Accurately estimating the regularization is key to the success of the reconstructed HR image. Suresh *et al.* [8] and Farsiu *et al.* [14] used the trial-and-error method or other additional procedures to determine the optimal parameter. In this case, the regularization parameter is expressed as a functional of the original image. Thus, (19) has the following alternative form

$$F(\vec{X}) = \arg\min_{\vec{X}} \left\{\sum_{k=1}^{n} \|\vec{Y}_k - DBF_k\vec{X}\|_2^2 + \lambda(\vec{X})V_\gamma(\vec{X})\right\} \quad (16)$$

A number of approaches for estimating the value of regularization parameter are based, such as the techniques of L-curve and cross validation. The L-curve and CV approaches can provide good solutions, but their computational costs are high. We have found that an effective and practical method of estimating the regularization parameter is using the method proposed in . Therefore, we will apply this method on our proposed generalized DAMRF-based SR model, but a little changed, to generate the optimum value of the regularization parameter adaptively, accurately, and efficiently. The regularization functional at each iteration step will contain the following properties [22].

i) $\lambda(\vec{X})$ is inversely proportional to $V_\gamma(\vec{X})$.
ii) $\lambda(\vec{X})$ is proportional to $\sum \|\vec{Y}_k - D_kB_kF_k\vec{X}\|_2^2$
iii) $\lambda(\vec{X}) > 0$.
iv) $\lambda(\vec{X})$ is influenced by the cross channel.

The assumption;

i) Controls the prior regularization term. With the progress of the iterative process, the value of the regularization term $V_\gamma(-\rightarrow X)$ increases, because high frequency is restored.
ii) Controls the data fidelity term. It is well known that the value of the data fidelity term is larger in images with large noise level than in images with small noise level. Therefore, the value of the regularization functional becomes larger as the data fidelity term becomes larger, which gives more weight on prior regularization term to suppress noise.

$$\lambda^n\vec{X}^{(n)} = \ln\left\{\tau\frac{\sum_{k=1}^{n}\left\|\vec{Y}_k - DBF_k\vec{X}^{(n)}\right\|_2^2}{V_\gamma\left(\vec{X}^{(n)}\right)+\delta} + 1\right\} \quad (17)$$

where $0 < \tau < 1$, $\lambda_n(\vec{X}_{(n)})$ is the regularization parameter at the nth iteration, and δ is guaranteed for the $V_\gamma(-\rightarrow X_{(n)})$ way from zero.

5.3 Optimization Using GNC

GNC is a good method to find the global solution for nonconvex minimization of the unconstrained problem [17]. Thus, in this paper, we use graduated nonconvexity optimization procedures to minimize the cost function (18). To derive the GNC update procedure for image estimation, we first compute the gradient of the cost function in (17) with respect to $\vec{X}$. This gradient is given by

$$\nabla F_1(\vec{X}) = \left\{\sum_{k=1}^{n} F_k^T B^T D^T (DBF_k\vec{X} - \vec{Y}_k) + \nabla\left(\lambda(\vec{X})V_\gamma(\vec{X})\right)\right\} \quad (18)$$

The GNC optimization procedure proposed in [22] can be briefly summarized here.

1. Use the cubic spline interpolation to calculate $X(0)$ as the initial guess of the HR image.
2. Set $\mu = \max i\ |X(0)(i) - X(0)(i-1)|$, and choose a convex $\gamma(0) \geq 2\mu$.
3. Update the state $X(n+1) = X(n) - \beta n\ \nabla F(X(n))$.
4. If $(\text{norm}(X(n+1) - X(n)) < \varepsilon)$, set $\gamma(n) = \max\{\Upsilon, \eta\gamma(n-1)\}$.

Here, β_n presents the step size at the nth iteration, and η is a factor for decreasing $\gamma(n)$ toward Y. proposed GDAMRF method, which is denoted as "GDAMRF," for SR reconstruction, it was evaluated in comparison with cubic spline interpolation and DAMRF method [8]. In our experiments, we consider images created by the reduction of resolution by a factor of 3.

6. Experiments

A number of experiments have been performed with the proposed algorithm. In this paper, we measure the performance of the proposed algorithms in terms of visual evaluation. To verify the effectiveness of our proposed GDAMRF method, this is denoted as "GDAMRF," for SR reconstruction.

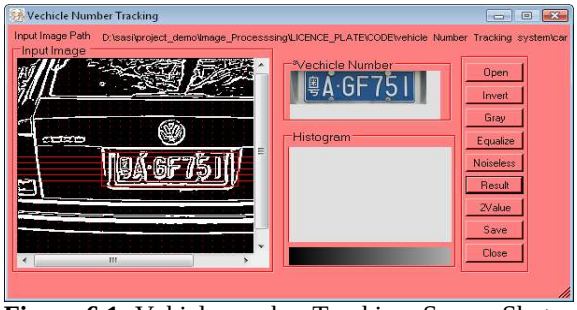

Figure 6.1: Vehicle number Tracking: Screen Shots.

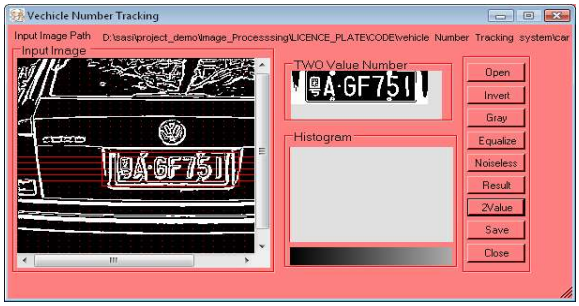

Figure 6.2: Vehicle number Tracking: Screen Shots.

7. Conclusion

In our present work, we have developed an effective method for localization of license plate regions from video snapshots of registered vehicles. The technique is extensively tested with 500 image samples and the gives satisfactory performance. One advantage of considering only vertical edges is due to fact that, the transverse motion of any car over the road makes some angle with the direction of the camera. This makes the vertical edges remain vertical but the other edges become skewed. This has made us running the same algorithm for the vehicles for which the frontal plane is inclined with the projection of the camera face to the vertical plane to the road. As the technique is edge based, the main limitation of our algorithm is that it performs well for less noisy images and having well printed characters over the license plates. That is why we have done some preprocessing task separately on some of the images. The technique can further be enhanced by applying some soft computing techniques for training the patterns of edge gradients. The localized license plate regions are to be subsequently processed by an effective *OCR* module for extraction of vehicle registration numbers.

8. Acknowledgments

Thanks to Prof. R. R. Nimbalkar for his valuable support & guidance.

References

[1] A Generalized DAMRF Image Modeling for Super resolution of License Plates, Weili Zeng and Xiaobo Lu, *IEEE* Transactions on Intelligent Transaction Systems, Vol.13,No.2, June2012
[2] C. N. E. Anagnostopoulos, I. E. Anagnostopoulos, I. D. Psoroulas. Loumos, and E. Kayafas, "License plate recognition from still images and video sequences: A survey," *IEEE Trans. Intell. Transp. Syst.*, vol. 9,
[3] no. 3, pp. 377–391, Sep. 2008.
[4] M. Protter, M. Elad, H. Takeda, and P. Milanfar, "Generalizing the nonlocal means to super resolution reconstruction," *IEEE Trans. Image Process.*, vol. 18, no. 1, pp. 36–51, Jan. 2009.
[5] F. J. Cortijo, S. Villena, R. Molina, and A. Katsaggelos, "Bayesian super resolution of text image sequences from low-resolution observations," in *Proc. IEEE Int. Symp. Signal Process. Appl.*, 2003, pp. 421–424.
[6] S. Chaudhuri and D. R. Taur, "High-resolution slow-motion sequencing—How to generate a slow-motion sequence from a bit stream," *IEEE Signal Process. Mag.*, vol. 22, no. 2, pp. 16–24, Mar. 2005.
[7] C. Miravet and F. B. Rodriguez, "A hybrid MLP-PNN architecture for fast image super-resolution," in *Proc. Int. Conf. Neural Inf. Process.*, 2003, pp. 417–424.
[8] S. Rajaram, M. D. Gupta, N. Petrovic, and T. S. Huang, "Learning based nonparametric image super-resolution," *EURASIP J. Appl. Signal Process.* vol. 2006, pp. 1–11, Jan. 2006.
[9] K. V. Suresh, G. M. Kumar, and H. N. Rajagopalan, "Super resolution of license plates in real traffic
[10] Zomet, A. Rav-Acha, and S. Peleg, "Robust super-resolution," in *Proc. IEEE Conf. Comput. Vis. Pattern Recog.*, 2001, vol. 1, pp. 645–650.
[11] W. F. Schreiber, *Fundamentals of Electric Imaging Systems*. NewYork: Springer-Verlag, 1986.
[12] C. Tomasi and R. Manduchi, "Bilateral filtering for gray and color images, "in *Proc. IEEE Int. Conf. Comput. Vis.*, New Delhi, India, Jan. 1998, pp. 836–846.
[13] D. Barash, "A fundamental relationship between bilateral filtering, adaptive smoothing, and the nonlinear diffusion equation," *IEEE Trans. Pattern Anal. Mach. Intell.*, vol. 24, no. 6, pp. 844–847, Jun. 2002.
[14] S. Farsiu, M. D. Robinsion, M. Elad, and P. Milanfar, "Fast and robust multiframe super-resolution," *IEEE Trans. Image Process.*, vol. 13, no. 10, pp. 1327–1344, Oct. 2004.
[15] M. Elad, "On the bilateral filter and ways to improve it," *IEEE Trans.Image Process.*, vol. 11, no. 10, pp. 1141–1151, Oct. 2002.
[16] M. Elad, "Retinex by two bilateral filters," in *Proc. 5th Int. Conf. Scale- Space PDE Comput. Vis.*, Hofgeismar, Germany, 2005, pp. 217–229
[17] S. Z. Li, *Markov Random Field Modeling in Computer Vision*. Tokyo, Japan: String-Verlag, 1995.
[18] S. P. Kim and W. Y. Su, "Recursive high-resolution reconstruction of blurred multiframe images," *IEEE*

Trans. Image Process., vol. 2, no. 4,pp. 534–539, Oct. 1993.
[19] S. Geman and D. Geman, "Stochastic relaxation, Gibbs distribution and the Bayesian restoration of images," *IEEE Trans. Pattern Anal. Mach. Intell.*, vol. PAMI-6, no. 6, pp. 721–741, Nov. 1984.
[20] J. Xu, S. Li, and M. Yu, "Car license plate extraction using color and edge information," in *Proc. Mach. Learn. Cyber.* 2004, vol. 6,pp. 3904–3907.
[21] R. C. Gonzalez and R. E. Woods, *Digital Image Processing*. Singapore: Pearson, 2003.
[22] E. S. Lee and M. G. Kang, "Regularized adaptive high-resolution image reconstruction considering inaccurate sub-pixel registration," *IEEE Trans. Image Process.*, vol. 12, no. 7, pp. 826–837, Jul. 2003.
[23] http://www.ieee.org/2011/05/13Generalized DAMRF Image Modeling
[24] http://www.sourceforge.com

Author Profile

Vikas Nivrutti Dhakane received B.E in Computer science & Engineering from Shivaji University in 2010 and also pursuing M. Tech, in JNTU. My areas of interest are System Programming, Networking and Cloud Computing.

Jalinder Nivrutti Ekatpure received B.E in Computer science & Engineering from Pune University in 2008 and also pursuing M.Tech, in JNTU. My areas of interest are Data Mining.